# Dual-Mode Quasi-Elliptic-Function Bandpass Filters Using Ring Resonators With Enhanced-Coupling Tuning Stubs

Lung-Hwa Hsieh, *Student Member, IEEE*, and Kai Chang, *Fellow, IEEE*

***Abstract*—A novel microwave dual-mode quasi-elliptic-function bandpass filter structure has been designed and fabricated. The filter uses $L$-shaped coupling arms for enhanced coupling and dual-mode excitation. The effects of varying the length of tuning stubs and gap size between tuning stubs and ring resonator have been studied. Filters using multiple cascaded ring resonators with high rejection band are presented. The new filters have been verified by simulation and measurement with good agreement.**

***Index Terms*—Bandpass filter, dual mode, enhanced coupling, quasi-elliptic function, ring resonator.**

## I. Introduction

THE microstrip ring resonator has been widely used to evaluate phase velocity, dispersion, and effective dielectric constant of microstrip lines. The main attractive features of the ring resonator are not only limited to its compact size, low cost, and easy fabrication, but also presents narrow passband bandwidth and low radiation loss. Many applications, such as bandpass filters, oscillators, mixers, and antennas using ring resonators have been reported [1]. Moreover, most of the established bandpass filters were built by dual-mode ring resonators, which were originally introduced by Wolff [2]. The dual-mode consists of two degenerate modes, which are excited by asymmetrical feed lines, added notches, or stubs on the ring resonator [1]–[3]. The coupling between the two degenerate modes is used to construct a bandpass filter. By proper arrangement of feed lines, notches, or stubs, the filter can achieve Chebyshev, elliptic, or quasi-elliptic characteristics. Recently, one interesting excitation method using asymmetrical feed lines with lumped capacitors at input and output ports to design a bandpass filter was proposed [4].

Low insertion loss, high return loss, and high rejection band are the desired characteristics of a good filter. However, a conventional end-to-side coupling ring resonator suffers from high insertion loss, which is due to the circuit's conductor, dielectric, radiation losses, and an inadequate coupling between feeders and the ring resonator. The size of the coupling gap between ring resonator and feed lines affects the strength of coupling and the resonant frequency [1]. For instance, for a narrow coupling gap size, the ring resonator has a tight coupling and can provide a low insertion loss, but the resonant frequency will be influenced greatly and for a wide gap size, the resonator has a high insertion loss and the resonant frequency is slightly affected. In order to improve the insertion loss, some structures have been published to enhance the coupling strength of ring resonators [5]–[8]. Several recent developments of the ring resonator using high-temperature superconductor (HTS) thin-film and micromachined circuit technologies have been presented [9]–[11]. This approach has the main advantage of very low conductor loss and, therefore, a low insertion loss is expected. In addition, some configurations are suggested to use active devices combined into the ring resonator to provide gain to compensate for the loss [12], [13]. In this paper, novel quasi-elliptic-function bandpass filters using microstrip ring resonators with low insertion loss have been developed. An $L$-shaped coupling arm was introduced to enhance the coupling and to generate perturbation for dual-mode excitation. The effects of the coupling gap and stub length have been studied. Filters using one , two, and three ring resonators are demonstrated and compared. These new types of bandpass filters have been verified by simulation and measurement. Both simulated and measured results exhibit good agreement.

## II. Dual-Mode Bandpass Filter Using a Single Ring Resonator

The basic structure of the proposed dual-mode filter is shown in Fig. 1(a). The square ring resonator is fed by a pair of orthogonal feed lines and each feed line is connected to an $L$-shaped coupling arm. Fig. 1(b) displays the scheme of the coupling arm that consists of a coupling stub and a tuning stub. The tuning stub is attached to the end of the coupling stub. As seen from the circuit layout, the tuning stub extends the coupling stub to increase the coupling periphery. In addition, the asymmetrical structure perturbs the field of the ring resonator and excites two degenerate modes [2]. Without the tuning stubs, there is no perturbation on the ring resonator and only a single mode is excited [14]. Comparing the new filter with conventional ones [1], which use perturbing notches or stubs inside the ring resonator, the conventional filters only provide dual-mode characteristics without the benefits of enhanced coupling strength and performance optimization.

The new filter was designed for the center frequency of 1.75 GHz and fabricated on a 50-mil-thick RT/Duroid 6010.2 substrate with a relative dielectric constant $\varepsilon_r = 10.2$. The length of the tuning stubs is $L$ and the gap size between the tuning stubs and ring resonator is $s$. The length of the

Manuscript received September 18, 2000.

The authors are with the Department of Electrical Engineering, Texas A&M University, College Station, TX 77843-3128 USA (e-mail: welber@ee.tamu.edu; chang@ee.tamu.edu).

Publisher Item Identifier S 0018-9480(02)04055-3.

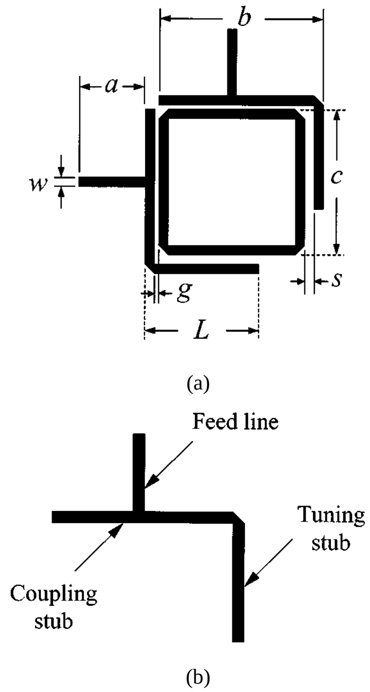


Fig. 1. New bandpass filter. (a) Layout. (b) $L$-shaped coupling arm.

feed lines is $a = 8$ mm, the width of the microstrip line is $w = 1.191$ mm for a 50-$\Omega$ line, the length of the coupling stubs is $b = 18.839{+}s$ mm, the gap size between the ring resonator and coupling stubs is $g = 0.2$ mm, and the length of one side of the square ring resonator is $c = 17.648$ mm. The dimension of the ring was designed for first-mode operation at the passband center frequency. The coupling gap $g$ was selected in consideration of strong coupling and etching tolerance. The simulation was completed using the IE3D electromagnetic simulator, which gives a full-wave solution using integral equations and the method of moments.[1]

By adjusting the length $L$ and gap size $s$ of the tuning stubs adequately, the coupling strength and the frequency response can be optimized. Single-mode excitation (Fig. 2) or dual-mode excitation (Fig. 3) can be resulted by varying $s$ and $L$. Figs. 2 and 3 show the measured results for five cases from changing the length $L$ of tuning stubs with a fixed gap size ($s = 0.8$ mm) and varying the gap size $s$ with a fixed length ($L = 13.5$ mm). Observing the measured results in Fig. 2, two cases for $L = 4.5$ and 9 mm with a fixed gap size only excite a single mode. The coupling between the $L$ arms and the ring can be expressed by external $Q\,(Q_e)$ as follows [15]:

$$Q_L = \frac{1}{2/Q_e + 1/Q_u} = \frac{f_o}{(\Delta f)_{3\text{ dB}}} \tag{1}$$

where $Q_L$ is the loaded $Q$, $Q_u$ is the unloaded $Q$ of the ring resonator, $f_o$ is the resonant frequency, and $(\Delta f)_{3\text{ dB}}$ is the 3-dB bandwidth. The unloaded $Q\,(Q_u = 137)$ for the square ring resonator can be obtained from the measurement using the circuit shown in Fig. 4. From (1), $Q_e$ is given by

$$Q_e = \frac{2Q_uQ_L}{Q_u - Q_L}. \tag{2}$$

[1]IE3D Version 6.1, Zeland Software Inc., Fremont, CA, 1998.

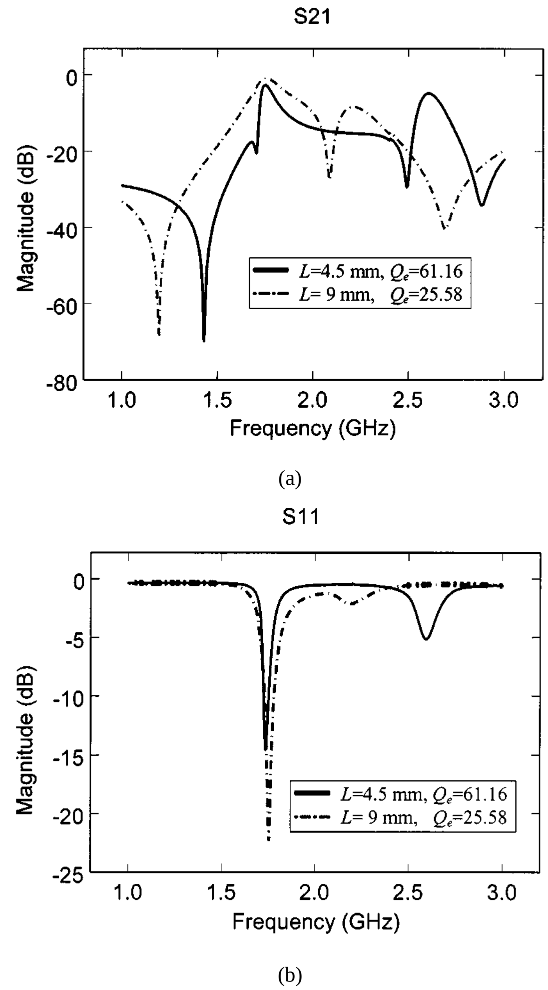


Fig. 2. Measured: (a) $S21$ and (b) $S11$ by adjusting the length of the tuning stub $L$ with a fixed gap size ($s = 0.8$ mm).

The performance for these two single-mode ring resonators is shown in Table I. On the other hand, the three cases shown in Fig. 3 by varying gap size $s$ with a fixed length $L = 13.5$ mm generate dual-mode characteristics. The coupling coefficient between two degenerate modes is given by [11]

$$K = \frac{f_{p2}^2 - f_{p1}^2}{f_{p2}^2 + f_{p1}^2} \tag{3}$$

where $f_{p1}$ and $f_{p2}$ are the resonant frequencies. In addition, the midband insertion loss $L_A$ corresponding to $Q_u$, $Q_e$, and $K$ can be expressed as [15]

$$L_A = 20\log\left[\frac{(1+Q_e/Q_u)^2}{2KQ_e} + \frac{KQ_e}{2}\right] \text{dB}. \tag{4}$$

The external $Q$ can be obtained from (4) through measured $L_A$, $K$, and $Q_u$. Moreover, the coupling coefficient between two degenerate modes shows three different coupling conditions. Let

$$K_o = 1/Q_e + 1/Q_u. \tag{5}$$

If the coupling coefficient satisfies $K > K_o$, then the coupling between two degenerate modes is overcoupled. In this overcoupled condition, the ring resonator has a hump response with a high insertion loss in the middle of the passband [16]. If

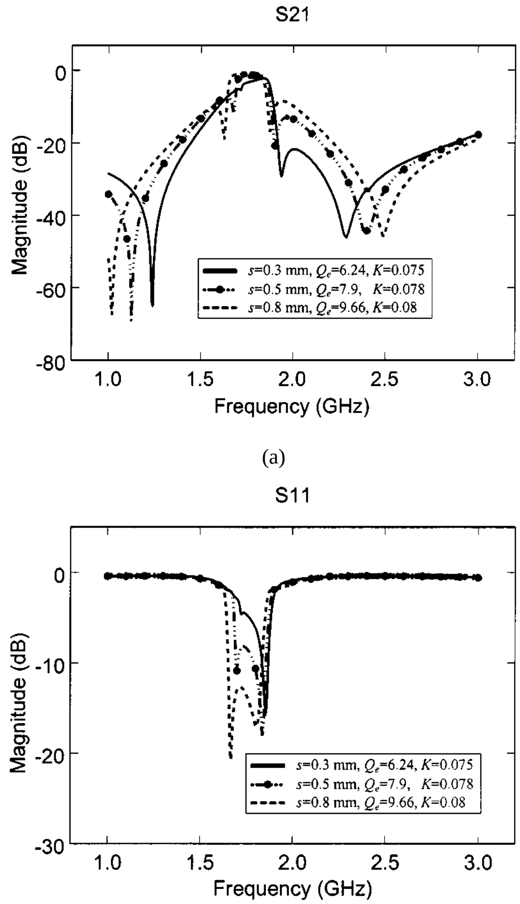


(b)

Fig. 3. Measured: (a) $S21$ and (b) $S11$ by varying the gap size $s$ with a fixed length of the tuning stubs ($L = 13.5$ mm).

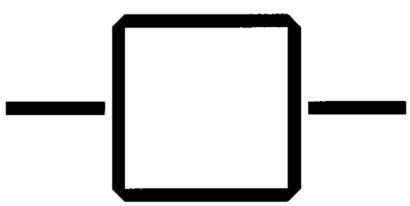

Fig. 4. Square ring resonator for the unloaded $Q$ measurement.

$K = K_o$, the coupling is critically coupled. Finally, if $K < K_o$, the coupling is undercoupled. For both critically and undercoupled coupling conditions, there is no hump response. Also, when the coupling becomes more undercoupled, the insertion loss in the passband increases [15]. The performance for the dual-mode ring resonators is displayed in Table II.

Observing the single-mode ring in Table I, it shows that a higher external $Q$ produces higher insertion loss and narrower bandwidth. On the other hand, for the dual-mode ring resonator in Table II, its insertion loss and bandwidth depend on the external $Q$, coupling coefficient $K$, and coupling conditions. For an undercoupled condition, the more undercoupled, the more the insertion loss and the narrower the bandwidth. To obtain a low insertion-loss and wide-band passband characteristic, the single-mode ring resonator should have a low external $Q$, which

TABLE I
SINGLE-MODE RING RESONATOR

| | Case1: $L$ = 4.5 mm, $s$ = 0.8 mm | Case2: $L$ = 9 mm, $s$ = 0.8 mm |
|---|---|---|
| Resonant Frequency $f_o$ | 1.75 GHz | 1.755 GHz |
| Insertion Loss IL | 2.69 dB | 0.97 dB |
| 3-dB Bandwidth | 70 MHz | 150 MHz |
| Loaded $Q$ | 25 | 11.7 |
| External $Q$ | 61.16 | 25.58 |

TABLE II
DUAL-MODE RING RESONATOR

| | Case 1: $L$ = 13.5 mm, $s$ = 0.3 mm | Case 2: $L$ = 13.5 mm, $s$ = 0.5 mm | Case 3: $L$ = 13.5 mm, $s$ = 0.8 mm |
|---|---|---|---|
| Resonant Frequencies ($f_{p1}$, $f_{p2}$) | (1.72,1.855) GHz | (1.7,1.84) GHz | (1.67,1.81) GHz |
| Coupling Coefficient $K$ | 0.075 | 0.078 | 0.08 |
| External $Q$ | 6.24 | 7.9 | 9.66 |
| Midband Insertion Loss IL | 2.9 dB | 1.63 dB | 1.04 dB |
| 3-dB Bandwidth | 160 MHz | 175 MHz | 192.5 MHz |
| Coupling Condition | undercoupled | undercoupled | undercoupled |

implies more coupling periphery between the feeders and ring resonator. Also, the dual-mode ring resonator can achieve the same performance by selecting a proper external $Q$ and coupling coefficient $K$ for an undercoupled coupling close to an overcoupled coupling.

Fig. 5 shows the simulated and measured results for the optimized quasi-elliptic bandpass filter. It can be found that an orthogonal-feed dual-mode ring resonator produces a quasi-elliptic characteristic [3], [17], [18]. As seen in Fig. 1, without the tuning stubs $L$, the fields of the ring are unaffected and the filter exhibits a stopband at the fundamental resonant frequency [1]. With the tuning stubs, the fields of the ring are perturbed and the ring can excite a dual mode. Also, two additional transmission zeros are generated. Both transmission zeros are located on either side of the passband [1], [17]. This frequency response is treated as a quasi-elliptic characteristic. In comparison of this new filer in Fig. 1 with the conventional filer, which is constructed by one-element hairpin [19], edge-coupled, and interdigital microstrips [15], the new filter can provide a quasi-elliptic characteristic with a wide bandwidth, while the conventional filter can only have a Chebyshev characteristic with a narrow bandwidth.

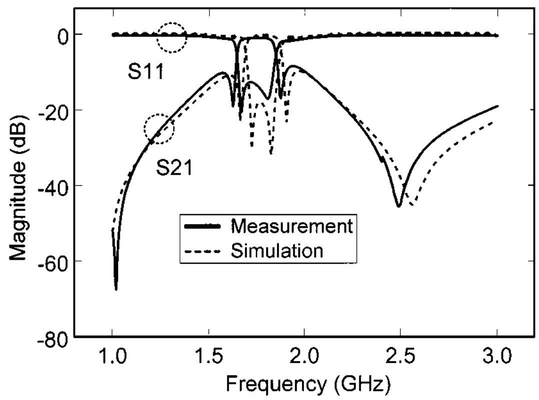


Fig. 5. Simulated and measured results for the case of $L = 13.5$ mm and $s = 0.8$ mm.

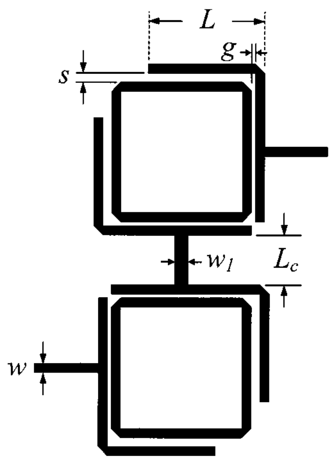


Fig. 6. Layout of the filter using two resonators with $L$-shaped coupling arms.

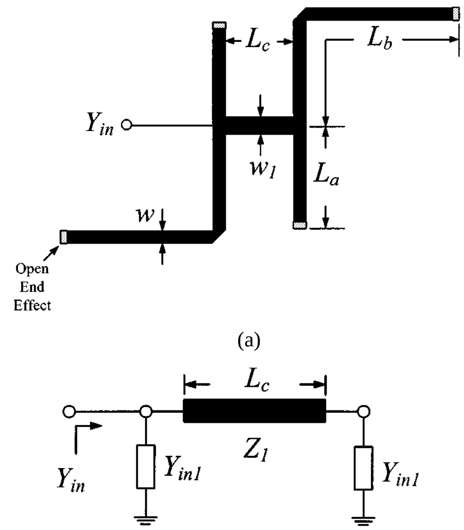


Fig. 7. Back-to-back $L$-shaped resonator. (a) Layout. (b) Equivalent circuit. The lengths $L_a$ and $L_b$ include the open-end effects.

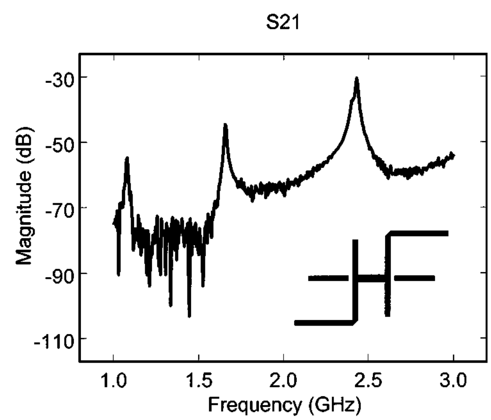


Fig. 8. Measured $S21$ for the back-to-back $L$-shaped resonator.

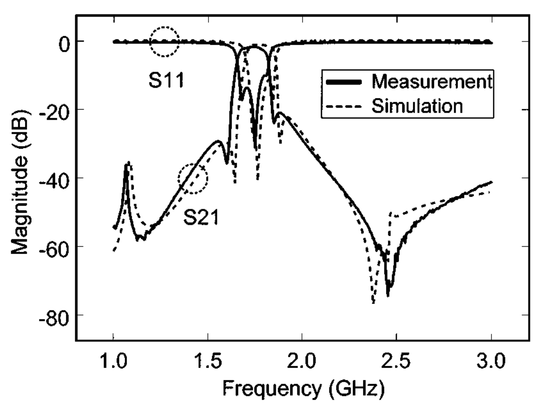


Fig. 9. Simulated and measured results for the filter using two resonators with $L$-shaped coupling arms.

## III. Dual-Mode Bandpass Filter Using Multiple Cascaded Ring Resonators

### *A. Dual-Mode Bandpass Filter Using Two Cascaded Ring Resonators*

Cascaded multiple ring resonators have advantages in acquiring a much narrower and sharper rejection band than the single ring resonator, and many bandpass filters using multiple ring resonators are fabricated by HTSs [9]–[11]. Fig. 6 illustrates the circuit composed of two ring resonators. This bandpass filter was built based on the $L = 13.5$ mm and $s = 0.8$ mm case of the single ring resonator of Fig. 1. Each filter section has the identical dimensions of the single ring resonator. A short transmission line $L_c$ of 6.2 mm with a width of $w_1 = 1.691$ mm connects to the coupling stubs to link the two ring resonators. The energy transfers from one ring resonator through the coupling and tuning stubs (or an $L$-shaped arm) and the short transmission line to another ring resonator. Observing the configuration for the $L$-shaped and short transmission line $L_c$ in Fig. 6, it not only perturbs the ring resonator, but can also be treated as a resonator. Considering this type resonator in Fig. 7(a), it is consisted of a transmission line $L_c$ and two parallel-connected open stubs. Its equivalent circuit is shown in Fig. 7(b). The input admittance $Y_{\mathrm{in}}$ is given by

$$Y_{\mathrm{in}} = Y_{\mathrm{in1}} + Y_1 \left[ \frac{Y_{\mathrm{in1}} + jY_1 \tan(\beta L_c)}{Y_1 + jY_{\mathrm{in1}} \tan(\beta L_c)} \right] \quad (6)$$

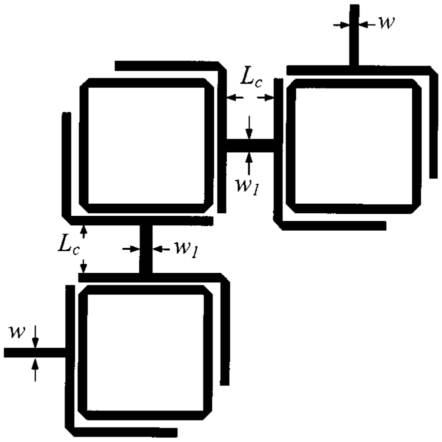


Fig. 10. Layout of the filter using three resonators with $L$-shaped coupling arms.

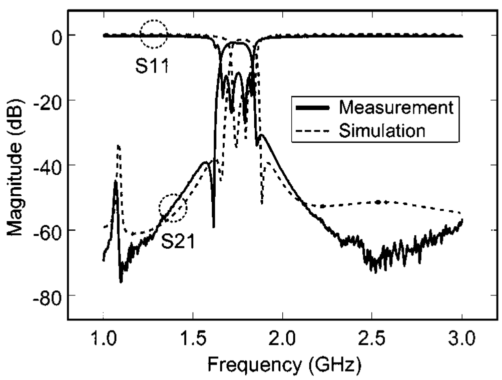


Fig. 11. Simulated and measured results for the filter using three resonators with $L$-shaped coupling arms.

where

$$Y_{\rm in1} = jY_o\left[\tan(\beta L_a) + \tan(\beta L_b)\right], \qquad \beta\text{: phase constant}$$
$$Y_1 = 1/Z_1, Y_o = 1/Z_o.$$

$Y_1$ is the characteristic admittance of the transmission line $L_c$, and $Y_o$ is the characteristic admittances of the transmission lines $L_a$ and $L_b$. Letting $Y_{\rm in} = 0$, the resonant frequencies of the resonator can be predicted. In Fig. 7, the resonant frequencies of the resonator are calculated as $f_{o1} = 1.067$, $f_{o2} = 1.654$, and $f_{o3} = 2.424$ GHz within 1–3 GHz. To verify the resonant frequencies, an end-to-side coupling circuit is built, as shown in Fig. 8. Also, the measured resonant frequencies can be found as $f_{mo1} = 1.08$, $f_{mo2} = 1.655$, and $f_{mo3} = 2.43$ GHz, which show a good agreement with calculated results.

Inspecting the frequency responses in Figs. 8 and 9, the spike at $f_{mo3} = 2.43$ GHz is suppressed by the ring resonators and only one spike appears at low frequency ($f_{mo1} = 1.08$ GHz) with a high insertion loss, which does not influence the filter performance. Furthermore, the resonant frequency ($f_{mo2} = 1.655$ GHz) of the resonator in Fig. 7 couples with the ring resonators. By changing the length $L_c$, the resonant frequencies will move to different locations. For a shorter length $L_c$, the resonant frequencies move to higher frequency and for a longer length $L_c$, the resonant frequencies shift to lower frequency. Considering the filter performance, a proper length $L_c$ should be carefully chosen. The filter has an insertion loss of 1.63 dB in the passband with a 3-dB bandwidth of 155 MHz.

TABLE III
FILTER PERFORMANCE

| | One ring Fig. 5 | Two rings Fig. 9 | Three rings Fig 11 |
|---|---|---|---|
| Minimum S21 | 1.04 dB | 1.63 dB | 2.39 dB |
| Frequency Range for S11< 10 dB | 1.655-1.835 GHz | 1.665-1.81 GHz | 1.685-1.83 GHz |
| 3-dB Bandwidth | 192.5 MHz | 155 MHz | 145 MHz |
| Fractional Bandwidth | 11 % | 8.9 % | 8.45 % |
| Band Rejection | Better than 10 dB | Better than 20 dB | Better than 30 dB |

### *B. Dual-Mode Bandpass Filter Using Three Cascaded Ring Resonators*

Fig. 10 illustrates the filter using three cascaded ring resonators. Any two of three resonators are linked by an $L$-shaped arm with a short transmission line $L_c$ of 6.2 mm with a width $w_1 = 1.691$ mm. The simulated and measured results are shown in Fig. 11. The filter has an insertion loss of 2.39 dB in the passband with a 3-dB bandwidth of 145 MHz. Table III summarizes the filter performance with one, two, and three ring resonators.

## IV. CONCLUSIONS

A novel type of microwave dual-mode filter using square ring resonators with an enhanced $L$-shaped coupling arm has been proposed. By changing the length of the tuning stubs and gap sizes between the tuning stubs and ring resonator, the insertion loss and frequency response of the filter can be optimized. To acquire a low insertion-loss and wide-band passband characteristic, the single-mode ring resonator should have stronger coupling between the feeders and ring resonator. Also, the dual-mode ring resonator should choose a proper external $Q$ and coupling coefficient $K$ to achieve the low insertion-loss and wide-band passband characteristics. Filters using cascaded ring resonators provide a sharp rejection band and narrow passband bandwidth with quasi-elliptic characteristics.

## ACKNOWLEDGMENT

The authors would like to thank C. Wang, Texas A&M University, College Station, for his technical assistance.

## REFERENCES

[1] K. Chang, *Microwave Ring Circuits and Antennas*. New York: Wiley, 1996, ch. 3, 7, and 12.
[2] I. Wolff, "Microstrip bandpass filter using degenerate modes of a microstrip ring resonator," *Electron. Lett.*, vol. 8, no. 12, pp. 163–164, June 1972.
[3] L. Zhu and K. Wu, "A joint field/circuit model of line-to-ring coupling structures and its application to the design of microstrip dual-mode filters and ring resonator circuits," *IEEE Trans. Microwave Theory Tech.*, vol. 47, pp. 1938–1948, Oct. 1999.
[4] I. Awai and T. Yamashita, "Two-stage bandpass filters based on rotated excitation of circular dual-mode resonators," *IEEE Microwave Guided Wave Lett.*, vol. 7, pp. 212–213, Aug. 1997.

[5] G. K. Gopalakrishnan and K. Chang, “Novel excitation schemes for the microstrip ring resonator with lower insertion loss,” *Electron. Lett.*, vol. 30, no. 2, pp. 148–149, Jan. 20, 1994.
[6] J. S. Hong and M. J. Lancaster, “Bandpass characteristics of new dual-mode microstrip square loop resonators,” *Electron. Lett.*, vol. 31, no. 11, pp. 891–892, May 1995.
[7] J. Y. Park and J. C. Lee, “A new enhanced coupling structure of microstrip ring resonator with two coupled lines and a slit,” in *IEEE MTT-S Int. Microwave Symp. Dig.*, 1998, pp. 805–808.
[8] W. C. Jung, H. J. Park, and J. C. Lee, “Microstrip ring bandpass filters with new interdigital side-coupling structure,” in *Asia–Pacific Microwave Conf.*, vol. 3, 1999, pp. 678–681.
[9] G. Tsuzuki, M. Suzuki, N. Sakakibara, and Y. Ueno, “Novel superconducting ring filter,” in *IEEE MTT-S Int. Microwave Symp. Dig.*, 1998, pp. 379–382.
[10] M. Reppel and H. Chaloupka, “Novel approach for narrowband super conducting filters,” in *IEEE MTT-S Int. Microwave Symp. Dig.*, 1999, pp. 1563–1566.
[11] F. Rouchaud, V. Madrangeas, M. Aubourg, P. Guillon, B. Theron, and M. Maignan, “New classes of microstrip resonators for HTS microwave filters applications,” in *IEEE MTT-S Int. Microwave Symp. Dig.*, 1998, pp. 1023–1026.
[12] L. Nenert, D. Denis, L. Billonnet, B. Jarry, and P. Guillon, “Analysis and optimization of noise and gain performances for various topologies of microwave ring resonator planar active filters,” in *IEEE MTT-S Int. Microwave Symp. Dig.*, 1999, pp. 1223–1226.
[13] A. Griol and J. Marti, “Microstrip multistage coupled ring active bandpass filters with harmonic suppression,” *Electron. Lett.*, vol. 25, no. 7, pp. 575–577, Apr. 1999.
[14] J. S. Hong and M. J. Lancaster, “Microstrip bandpass filter using degenerate mode of a novel meander loop resonator,” *IEEE Microwave Guided Wave Lett.*, vol. 5, pp. 371–372, Nov. 1995.
[15] G. L. Matthaei, L. Young, and E. M. T. Jones, *Microwave Filters, Impedance-Matching Networks, and Coupling Structures*. New York: McGraw-Hill, 1980, ch. 10 and 11.
[16] J. S. Hong and M. J. Lancaster, “Bandpass characteristics of new dual-mode microstrip square loop resonators,” *Electron. Lett.*, vol. 31, no. 11, pp. 891–892, May 1995.
[17] K. K. M. Cheng, “Design of dual-mode ring resonators with transmission zeros,” *Electron. Lett.*, vol. 33, no. 16, pp. 1392–1393, July 1997.
[18] L. H. Hsieh and K. Chang, “Compact dual-mode elliptic-function bandpass filter using a single ring resonator with one coupling gap,” *Electron. Lett.*, vol. 36, no. 19, pp. 1626–1627, Sept. 2000.
[19] M. Sagawa, K. Takahashi, and M. Makimoto, “Miniaturized hairpin resonator filters and their application to receiver front-end MIC,” *IEEE Trans. Microwave Theory Tech.*, vol. 37, pp. 1991–1997, Dec. 1989.

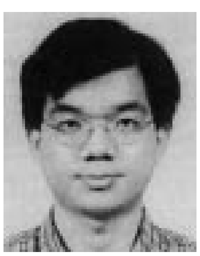

**Lung-Hwa Hsieh** (S’01) was born in Panchiao, Taiwan, R.O.C., in 1969. He received the B.S. degree in electrical engineering from the Chung Yuan Christian University, Chungli, Taiwan, R.O.C., in 1991, the M.S. degree in electrical engineering from the National Taiwan University of Science and Technology, Taipei, Taiwan, R.O.C., in 1993, and is currently working toward the Ph.D. degree in electrical engineering at Texas A&M University, College Station.

From 1995 to 1998, he was a Senior Design Engineer at General Instrument, Taipei, Taiwan, R.O.C., where he was involved in RF video and audio circuit design. Since 2000, he has been a Research Assistant with the Department of Electrical Engineering, Texas A&M University. His research interests include microwave integrated circuits and devices.

**Kai Chang** (S’75–M’76–SM’85–F’91) received the B.S.E.E. degree from the National Taiwan University, Taipei, Taiwan, R.O.C., in 1970, the M.S. degree from the State University of New York at Stony Brook, in 1972, and the Ph.D. degree from The University of Michigan at Ann Arbor, in 1976.

From 1972 to 1976, he was with the Microwave Solid-State Circuits Group, Cooley Electronics Laboratory, The University of Michigan at Ann Arbor, where he was a Research Assistant. From 1976 to 1978, he was with Shared Applications Inc., Ann Arbor, MI, where he was involved with computer simulation of microwave circuits and microwave tubes. From 1978 to 1981, he was with the Electron Dynamics Division, Hughes Aircraft Company, Torrance, CA, where he was involved in the research and development of millimeter-wave solid-state devices and circuits, power combiners, oscillators, and transmitters. From 1981 to 1985, he was with TRW Electronics and Defense, Redondo Beach, CA, where he was a Section Head involved with the development of state-of-the-art millimeter-wave integrated circuits and subsystems, including mixers, voltage-controlled oscillators (VCOs), transmitters, amplifiers, modulators, upconverters, switches, multipliers, receivers, and transceivers. In August 1985, he joined the Electrical Engineering Department, Texas A&M University, College Station, as an Associate Professor, and became a Professor in 1988. In January 1990, he became an E-Systems Endowed Professor of Electrical Engineering. He has authored and co-authored several books, including *Microwave Solid-State Circuits and Applications* (New York: Wiley, 1994), *Microwave Ring Circuits and Antennas* (New York: Wiley, 1996), *Integrated Active Antennas and Spatial Power Combining* (New York: Wiley, 1996), and *RF and Microwave Wireless Systems* (New York: Wiley, 2000). He has served as the Editor of the four-volume *Handbook of Microwave and Optical Components* (New York: Wiley, 1989 and 1990). He is the Editor of *Microwave and Optical Technology Letters* and the Wiley Book Series on “Microwave and Optical Engineering.” He has also authored or co-authored over 350 technical papers and several book chapters in the areas of microwave and millimeter-wave devices, circuits, and antennas. His current interests are in microwave and millimeter-wave devices and circuits, microwave integrated circuits, integrated antennas, wide-band and active antennas, phased arrays, microwave power transmission, and microwave optical interactions.

Dr. Chang was the recipient of the 1984 Special Achievement Award presented by TRW, the 1988 Halliburton Professor Award, the 1989 Distinguished Teaching Award, the 1992 Distinguished Research Award, and the 1996 Texas Engineering Experiment Station (TEES) Fellow Award presented by Texas A&M University.